Circulation pattern control of wet days and dry days in Free State, South Africa

Chibuike Chiedozie Ibebuchi (chibuike.ibebuchi@uni-wuerzburg.de)
Julius Maximilians University Würzburg: Julius-Maximilians-Universitat Wurzburg
https://orcid.org/0000-0001-6010-2330

Original Article

Keywords: Atmospheric circulation, southern Africa, Free State, circulation types, principal component analysis, rainfall

Posted Date: February 4th, 2021

DOI: https://doi.org/10.21203/rs.3.rs-160597/v1

Abstract

Atmospheric circulation is a vital process in the transport of heat, moisture, and pollutants around the globe. The variability of rainfall depends to some extent on the mechanisms of atmospheric circulation. This paper uses the concept of classifying the recurrent large-scale atmospheric circulation patterns in southern Africa, and the linkage of the classified patterns to wet days and dry days in Free State, South Africa, for the analysis of how the probability of wet and dry events in Free State can be associated with specific synoptic situations, in addition to the underlying dynamics. Principal component analysis was applied to the T-mode matrix (column/variable is time series and row is grid points at which the field was observed) of daily mean sea level pressure field from 1979 to 2018 in classifying the recurrent circulation patterns in southern Africa. 18 circulation types (CTs) were classified in the study region. From the linkage of the CTs to the observed rainfall data, from 11 stations in Free State, it was found that dominant austral winter and late austral autumn CTs have a higher probability of bringing dry days to Free State. Dominant austral summer and late austral spring CTs were found to have a higher probability of bringing wet days to Free State. Cyclonic/anti-cyclonic activity over the southwest Indian Ocean, explained to a good extent, the inter-seasonal variability of rainfall in Free State. The synoptic state associated with a stronger anti-cyclonic circulation at the western branch of the South Indian Ocean high-pressure, during austral summer, leading to enhanced moisture transport by southeast winds was found to have the highest probability to bring above-average rainfall in most regions in Free State; while the synoptic state associated with enhanced transport of cold dry air, from the Benguela current, by the extratropical westerlies was found to be associated with the highest probability of (winter) dryness in Free State.

1 Introduction

The forecast ability of surface variables such as rainfall is of core interest in climatology. According to Vicente-Serrano and López-Moreno (2006), the linkage of large-scale circulation patterns to a surface variable explains in physical terms the intensity and spatial distribution of the surface variable. In the regional context of Free State, southern Africa, this paper examines how specific synoptic situations can be used to forecast the probability of wet and dry events.

The concept of synoptic climatology deals with the connection between large-scale atmospheric circulations and local surface variables. It involves the classification of the recurrent circulation patterns in a region, and the linkage of the classified patterns to the variability of surface variables in a local region, for example in Andorra (Esteban et al. 2015), in the whole Pyrenees (Lemus-Canovas et al. 2019a); in Austria (Sibert et al. 2007) among many others. When used to explain surface variables, classification of recurrent circulation patterns can be considered as a method of statistical downscaling (Maraun and Widmann 2018), which involves the correlation of clustered days with a similar spatial pattern, to a large-scale atmospheric variable. Linking atmospheric circulation to local surface variables in the

Mediterranean region, Maheras and Kolyva-Machera (1990) noted that zonal recurrent circulation patterns are associated with dry periods whereas meridional recurrent circulation patterns are associated with humid periods.

This paper uses the concept of obliquely rotated principal component analysis (PCA), on the T-mode matrix of a climatic variable that explains atmospheric circulation (Richman 1981; Martin-Vide et al. 2008), in obtaining the circulation types in southern Africa. For the characterization of how the mechanism of the individual circulation types could predict rainfall in Free State, the concept of moisture flux convergence (Kuo 1965), will be incorporated in the analysis. Several researchers have found that the parameterization of convective rainfall could be well linked to the concept of moisture convergence (Sylla et al. 2011; Loriaux et al. 2017).

The focus of this paper is thus structured as follows:

1. principal component analysis will be used as an eigenvector based classification tool to obtain the recurrent circulation patterns in southern Africa.
2. physically motivated correlation between the mechanism of the recurrent patterns and rainfall variability in Free State will be investigated.

2 Data And Methodology

Classification of circulation patterns was achieved with gridded reanalysis mean sea level pressure (SLP) dataset, from the European Center for Medium-Range Weather Forecasts (ECMWF), ERA-Interim (Dee et al. 2011). The original temporal resolution is 6 hourly data, from 1979 to 2018. Daily averages were computed, for the complete analysis period. The horizontal resolution of the ERA-Interim SLP dataset is. The spatial coordinate for the circulation typing is 5.25°E-55.25°E and 6°S-50.25°S. Daily rainfall data from 11 stations in Free State, obtained from http://www.dwa.gov.za/Hydrology/Verified/hymain.aspx, for the 1979-2018 period, was used in characterizing the rainfall characteristics of the recurrent patterns in Free State, South Africa (Fig. 1). The dotted red lines in Fig. 1 are the geographical locations of the selected rainfall stations in Free State.

For the classification of the recurrent patterns in southern Africa, obliquely rotated principal component analysis (PCA) was applied to the T-mode matrix of daily z-score standardized SLP field in southern Africa. The decision to represent the matrix in a T-mode structure is based on the finding that obliquely rotated PCA on the T-mode matrix of a field that explains atmospheric circulation is an optimal classification procedure, for the representation of the basic temporal modes of variability associated with a climatic variable that explains atmospheric circulation, in terms of recurrent patterns (Richman 1986; Compagnucci and Richman 2008). Richman and Lamb (1985) noted that rotated PCA on the T-mode field results in a simplified time-series isolating subgroups of observations with a coherent spatial pattern. In the classification process, a correlation matrix was used, which yielded correlation coefficients between

pairs of daily time observations in the study period, which constituted 14610 observations. Singular value decomposition was used in factorizing the correlation matrix to obtain the eigenvalues and the eigenvectors. The selection of the optimal number of components to retain was based first, on scree-test (Cattel 1966; Wilks 2006). This was helpful to have an idea of the range of possible optimal number of components to retain for the analysis - based on cutting the component numbers after a relatively small slope is followed by a noticeable drop. The discarded components have typically low and close eigenvalues in line with the recommendation of North et al. (1982) on ensuring the separability of eigenvalues of the retained components. However, since Preisendorfer et al. (1981) noted that a few of the discarded components might contain meaningful information necessary for the research goal; sensitivity analysis was applied for the optimization of the number of components to retain. The sensitivity analysis ensures that the addition of a further component uncovers a new pattern that has not been already delineated by previous vectors; this was statistically approached by ensuring that the congruence coefficient between the new input pattern (i.e. component score) and the already classified input patterns is low (Richman 1981).

Richman and Lamb (1985) recommended that multiplying the eigenvectors by the square root of their corresponding eigenvalues makes them more responsive to rotation; hence the retained eigenvectors were further loaded with the square root of their corresponding eigenvalues which makes them longer than a unit length henceforth referred to as loadings. To simplify the structure of the eigenvector loadings, they were rotated obliquely using Promax at a power of 2 ((Richman 1986). The oblique rotation maximizes the number of near-zero loadings so that each retained component clusters a unique number of variables that a general influence can be attributed to (Richman 1981). Also, the decision of using oblique rotation was to ensure that orthogonality constraint does not lead to artificial physical features in the classification (Richman 1981; Wilks 2006). The component scores present the input spatial patterns localized in time by the eigenvector loadings, and loadings (time-steps) that are near zero do not contribute to the PC sores (Compagnucci and Richman 2008). The absolute value of the loadings represent a vital signal, and for a given retained component, further clustering of the component loadings into negative high loadings and positive high loadings using a specified threshold will decrease the internal distances among classes so that there is greater similarity between days grouped under a given class (Richman and Gong 1999). Thus each component yields two classes and the SLP composite of the days grouped under a class is the circulation type (CT). Richman and Gong (1999) recommended that threshold values within the range of 0.2-0.35 will be sufficient to separate the PCs, here was used.

For the linkage of the CTs, classified in this paper, to rainfall variability in Free State, wet days clustered under each CT, were characterized as the count of days, per station, with rainfall greater than 0.3mm (Brisson et al. 2011; Plavcova et al. 2013). Polade et al. (2014) characterized dry days as days with precipitation less than 1mm. In this work, dry days were characterized, as the count of days with rainfall less than 1mm at the complete 11 selected stations.

The rainfall characteristics of each CT, concerning the probability of being associated with dry days and wet days, were calculated using Eq. 1 and 2, respectively.

$$P_{d_i} = \frac{d_i}{N_i} \times 100 \quad i = 1 \ldots n$$

(1)

$$P_{w_i} = \frac{w_i}{N_i} \times 100 \quad i = 1 \ldots n$$

(2)

P_{d_i} is the percentage of dry days for a given CT; d_i is the total number of dry days for the CT in question; N_i is the total number of days clustered under a given CT. P_{w_i} is the percentage of wet days in a given CT, and w_i is the total number of wet days for the CT in question (for each of the 11 stations) and n is the number of CTs classified.

3 Study Regions

Southern Africa is located between three oceans – the Southern Ocean, the South Atlantic Ocean, and the South Indian Ocean. The western subtropical regions of Southern Africa are relatively drier than the eastern regions due to the influence of the cold Benguela current. Rainfall is mostly in austral summer (DJF), except for the southernmost regions of South Africa that are characterized by the Mediterranean climate. The local study region, Free State (Fig. 1), is a province in South Africa. Its attitude is about 1600m above sea level. The escarpment at the eastern regions of Free State is steeper relative to the western regions. Free State is characterized by hot summers and cold winters; also, rainfall is much common in the summer months.

Rainfall variability in southern Africa is influenced by a low level (at about 850hPa) land-based convergence zone (Tyson 1986; Cook 2000; Ninomiya 2008; Lazenby et al. 2016), called the South Indian Ocean Convergence Zone (SICZ). The SICZ extends off the southeast coast of southern Africa (Fig. 2).

Fig. 2 shows some of the basic synoptic rainfall producing systems that are typically captured in the modes of large-scale atmospheric circulations, in southern Africa. Variability in these systems modulates the strength and location of the SICZ. Relaxation of trade winds during the austral warm seasons, at the region of the Angola warm current, lead to the development of a warm pool in the region (Reason and Smart 2015). Moisture flux from the warm pool feeds into the Angola low, which is both a heat low and a tropical low during austral summer (Munday and Washington 2017). During austral summer, moisture from the cross-equatorial northeast trade wind also feeds into the Angola low. The cyclonic circulation associated with the Angola low transports moisture from the warm pool and the tropical Indian Ocean to

the (eastern) subtropical regions of southern Africa. According to Viguad et al. (2009), the ITCZ modulates the SICZ through the Angola low – the sustenance of the Angola low can be related to the enhancement of the ITCZ. Another heat low termed the Kalahari low develops at the western subtropical region in response to diabatic heating.

The anti-cyclonic circulation at the South Indian Ocean high-pressure strengthens southeast winds, and thus enhances moisture advection into southern Africa from the southwest Indian Ocean. Low-level convergence of the moisture from the southwest Indian Ocean advected by easterly winds and the moisture advected from the tropical South Atlantic Ocean (warm pool) by the circulation at the Angola low, create the foundation zone of the SICZ (Cook 2000). Also, moisture convergence in the SICZ can be supported by the moisture advected as a result of the migratory mid-latitude cyclones. According to (Cook 2000) the Agulhas current equally influences the SICZ through the enhanced evaporation in the region, moreover, rainfall variability in South Africa is also modulated by sea surface temperature (SST) anomalies at the Agulhas current (Walker 1990).

Sylla et al. (2011) noted that diabatic heating and moisture convergence are two phenomena that lead to deep conditional instability, which enhances convective rainfall. Enhanced diabatic heating, leads to the formation of a thermal tower (typically at the western regions of southern Africa), known as the continental tropical low. The continental tropical low is associated with enhanced vertical velocity and convective instability. Thus in the presence of adequate moisture at the boundary layer, its occurrence normally correlates with enhanced rainfall in southern Africa. Cook (2000) noted that the variability in the strength and position of the South Indian Ocean high-pressure and continental heating are the major factors that affect the position and strength of the SICZ.

In the Mozambique Channel, a cyclonic circulation prominent in austral summer plays a vital role in the hydroclimate of southern Africa. The system is termed the Mozambique Channel Trough. During its active stage rainfall is enhanced at northern Mozambique and Madagascar but diminished in southern African mainland (Barimalala et al. 2019) due to enhanced evaporation in the Channel and the adjustment of moist easterly winds to westerly by the strong cyclonic circulation in the Channel. Finally, during austral winter (JJA) the northward track of the mid-latitude cyclones allows cold fronts to sweep across the regions with the Mediterranean climate leading to enhanced winter rainfall in the regions (e.g. Western Cape).

4 Results

4.1 Circulation types in southern Africa

The application of the scree-test for the decision of the optimal number of components to retain, as shown in Fig. 3, suggests retaining 6 to 8 components. However, in line with the findings of Preisendorfer et al. (1981), the sensitivity analysis led to retaining 9 (optimal) components.

Fig. 4 shows the SLP composites (i.e. CTs) classified in the study region. Each retained component yields two CTs; hence there is a total number of 18 CTs. Fig. 5 shows the relative monthly frequency of occurrence for each CT in Fig. 4. In as much as it is common for any of the CTs to occur at any time of the year, the CTs can be further classified with respect to their dominance in either austral winter/autumn season or austral summer/spring season. CT1, CT6, CT7, CT9, CT11, CT14, and CT16 can be grouped as winter/autumn recurrent patterns, with CT9 and CT11 extending dominance into early austral spring (September/October); generally, they can be analogous to CTs associated with cold seasons. Similarly, CT2, CT3, CT5, CT8, CT10, CT12, CT13, CT15 and CT18 can be grouped as austral summer/spring recurrent patterns; their dominant periods are within the range of October (late austral spring) to February (late austral summer), with CT5, CT2, and CT3 extending dominance into early austral autumn (March/April). The occurrence of CT4 was a bit mixed up; it has a high probability to occur, almost homogenously, at any time of the year. CT17 is specifically an austral spring dominant pattern. In general, CT2, CT5, CT8, CT10, CT12, CT13, CT15, CT18 can be grouped as warm-season recurrent patterns.

The probability of occurrence of the CTs (Fig. 6) was calculated as the ratio of the number of days clustered under the CT to the total number of days in the study period (i.e. 14610 days). CT1 is the most occurred cold season CT in the study period, followed by CT9. CT5 similarly, is the most occurred warm-season CT, followed by CT8. CT5 is the austral summer climatology of atmospheric circulation in the study region. CT12 and CT18 are relatively rare CTs. CT1 is close to the climatological mean state of SLP field variability in the study region (Molteni et al. 1990).

The oblique rotation allows inter-correlation between the component scores, and also a day might have high loadings (>0.2) under more than one retained component so that the classification procedure allows for the grouping of a day under more than one CT, which logically implies the CTs that reoccurred on the day in question. Since the classified data is continuous it is justified that more than one day is assigned to a CT. As a result, the sum of the percentages in Fig. 6 does not add up to 100%. Atmospheric circulation is a continuum and this justifies the relaxation of a rigid grouping (e.g. K-means clustering), which allows a day to be classified under only one CT. CT1, CT4, CT5, and CT8 were found to relatively have a higher probability to occur; Harr and Elsberry (1995) explained such CTs as nearly constant recurrent patterns that have slowly varying features; the external distances among the classes were satisfactorily large except with aforementioned CTs.

4.2 Linkage of wet and dry days in Free State to the circulation types

The probability of dry days and wet days in each CT was calculated using Eq. 1 and 2 respectively. The probability of dry days in each of the 18 CTs can be visualized in Fig. 7. Recall that CT1, CT6, CT7, CT9, CT11, CT14, and CT16 were categorized as cold season CTs. Fig. 7 shows that these recurrent patterns have, relatively, the higher chances of bringing dry days to Free State, when they occur. Generally, the inference is that cold season dominant CTs are associated with a higher possibility of dry days in Free State. According to Reason and Mulenga (1999), the reason is that SST anomalies at the southwest

Indian Ocean influences the inter-seasonal rainfall variability in most regions of South Africa; they linked dry days in South Africa to the cooling of SST at the southwest Indian Ocean – which is a common phenomenon in the cold season CTs. From Fig. 4, for the aforementioned cold season CTs, anti-cyclonic circulation dominates over the southwest Indian Ocean. Anti-cyclonic circulation is normally associated with the less convective activity (Harr and Elsberry 1995). CT6 and CT14 have the highest probability to bring dry days in Free State; Fig. 8 also shows that relatively, there is generally a low possibility of wet days when either of these CTs occurs; supporting the fact they are truly dry synoptic situations in Free State.

Fig. 10 shows the SLP field, moisture flux, and convergence field during CT6 and CT14. Under CT14 a high-pressure system and associating divergence are evident over Free-state and the Greater Agulhas region, leading to subsidence (rainfall suppression), and reduction of convective activity at the Agulhas current which is a principal source of moisture to South Africa, respectively. Under CT6, the mid-latitude cyclone strengthens and tracks further north so that westerly wind is enhanced in the advection of cold drier to Free State. Hence at the synoptic scale, enhanced dryness in Free State can be attributed to large-scale subsidence, suppression of convection at the Greater Agulhas region, and advection of cold dry air by extratropical westerly winds, from the Benguela region.

From Fig. 7, for the warm season CTs, i.e. CT2, CT3, CT5, CT8, CT10, CT12, CT13, CT15, and CT18, the probability of dry days in these CTs are generally less, relative to the cold season CTs. Fig. 8 shows the probability of each CT to bring wet days across all the eleven selected stations. The distribution portrayed by the box-plots also helps in understanding the strength of each CT to bring a homogeneous or heterogeneous number of wet days across the 11 stations (jointly considered). Take for example; the exceptional skewness of CT15 indicates that its mechanism makes it bring (enhanced) rainfall in specific regions only.

For the eleven selected stations in Free State, Fig. 9 shows the regions under the dominant influence of a given CT, based on having the highest probability of bringing wet days (Fig. 9a) and the probability of bringing extreme rainfall (Fig. 9b). An extreme rainfall day for each CT was characterized as the count of days with daily rainfall amount greater than the 99 percentile rainfall value, per station. Fig. 8 and Fig. 9 show that CT12 has the highest chances of bringing widespread extreme rainfall to most regions in Free State when it occurs. Southwestern regions in Free State are more likely to be influenced by the dynamics of CT15. Some regions are under the influence of CT13. However, the application of the classification scheme to other SLP gridded data set (not shown) reproduced all the CTs with the exception of CT13, suggesting that it might be an artifact of ERA-Interim. Hence more focus will be placed on CT15.

From Fig.10, at the synoptic scale, extreme rainfall in most regions in Free State under CT12 can be attributed to the strengthening of the South Indian Ocean high-pressure leading to enhanced advection of moisture by the southeast wind. Also, the offshore movement of the thermal low into the South Atlantic Coast implies moistening of the western subtropical boundary layer, weakening of the South Atlantic Ocean high-pressure, and enhanced convergence in the region, so that more moisture is available to be

advected into Free State by westerly winds. On the other hand, CT15 reflects enhanced convergence of moist winds from the Angola warm current and cross-equatorial trade wind into the Angola low. The western branch of the South Indian Ocean high-pressure is equally weakened so that fewer southeast winds penetrate Free State compared to CT12; however, the continental tropical low evident in this synoptic situation, coupled with the enhanced cyclonic activity at the Agulhas region, and the enhanced convergence at the Angola low are generally favourable for the enhancement of deep convection at preferred regions in Free State. In general, extreme rainfall in Free State can be attributed to enhanced transport of moisture by southeast and southwest winds into the local study region; the formation of continental tropical lows at the western regions of southern African, coupled with enhanced cyclonic activity at the Agulhas current.

5 Conclusions

In this study, the CTs in southern Africa were classified and linked to rainfall variability in Free State, South Africa. The CTs associated with the higher probability of bringing wet days and dry days to Free State were noted. The mechanisms, in the light of moisture flux and convergence, through which the selected CTs can influence the intensity and spatial variability of rainfall across 11 stations in Free State were equally analyzed.

Using obliquely rotated PCA on the T-mode matrix of SLP data set (Richman 1981), 18 CTs were classified and each CT was found to be related to the probability of a specific weather event. CTs dominant in austral summer and austral late spring – when SST is high at the southwest Indian Ocean - were found to be associated with a higher possibility of bringing wet days to Free State; whereas austral winter and austral late autumn dominant CTs - when SST is low at the southwest Indian Ocean - were found to be associated with a higher possibility of bringing dry days to Free State, in line with the finding of Reason and Mulenga (1999) that SST anomalies at the southwest Indian Ocean explain to a good extent the inter-seasonal variability of rainfall in South Africa.

The synoptic situation associated with the highest probability of wet days and extreme wet days in Free State is characterized by stronger circulation at the South Indian Ocean high-pressure leading to the enhanced transport of moisture from the southwest Indian Ocean by southeast winds; it equally features moistening of the Benguela current. According to Lazenby et al. (2016), stronger circulation at the South Indian Ocean high-pressure during austral summer correlates with the strengthening of the SICZ and enhanced rainfall in southern Africa. On the other hand, the occurrence of continental tropical lows and enhanced cyclonic activity at the Agulhas region was equally found to cause enhanced rainfall in some regions in Free State.

Finally, enhanced dry conditions in Free State can be attributed to large-scale subsidence (Dedekind et al. 2016), suppression of convection at the Greater Agulhas region (Reason 2001), and advection of cold dry air from the Benguela region to Free State, by the extratropical westerly wind.

Declarations

Conflict of interest: There are no conflicts of interest in this paper

Funding statement: This research received no specific grant from any funding agency in the public, commercial, or not-for-profit sectors.

Author's contribution: work was designed and executed by Chibuike Chiedozie Ibebuchi

References

1. Barimalala R, Blamex RC, Desbiolles F, Reason CJC (2019) Variability in the Mozambique Channel Trough and impacts on Southeast African rainfall. J Clim 33 2:749-765. https://doi.org/10.1175/JCLI-D-19-0267.1
2. Brisson E, Demuzere M, Kwakernaak B, Van-Lipzig NP (2011) Relations between atmospheric circulation and precipitation in Belgium. Meteorol Atmos Phys 111 1:27–39. https://doi.org/10.1007/s00703-010-0103-y
3. Cattell RB (1966) The Scree Test for the Number of Factors. Multivar Behav Res 1 2:245–276. https//doi:10.1207/s15327906mbr0102_10
4. Compagnucci RH, Richman MB (2008) Can principal component analysis provide atmospheric circulation or teleconnection patterns? Int J Climatol 28 6:703–726. https://doi.org/1002/joc.1574
5. Cook KH (2000) The South Indian Convergence Zone and Interannual Rainfall Variability over Southern Africa. J Clim 13 21:3789–3804. https://doi.org/10.1175/1520-0442(2000)013<3789:TSICZA>2.0.CO;2
6. Dedekind Z, Engelbrecht FA, Merwe J (2016) Model simulations of rainfall over southern Africa and its eastern escarpment. Water SA 42 1:129. http://dx.doi.org/10.4314/wsa.v42i1.13
7. Dee DP, Uppala SM, Simmons AJ, et al (2011) The ERA-interim reanalysis: configuration and performance of the data assimilation system. Q J R Meteorol Soc 137 656:553-597. https://doi.org/10.1002/qj.828
8. Esteban P, Jones PD, Martin-Vide J, Mases M (2005) Atmospheric circulation patterns related to heavy snow days in Andorra, Pyrenees. Int J Climatol 25 3:319-329. https://doi.org/10.1002/joc.1103
9. Harr AP, Elsberry RL (1995) Large-scale circulation variability over the Tropical Western North Pacific. Part 1: spatial patterns and tropical cyclone characteristics. Mon Weather Rev 123 5:1225–1246. https://doi.org/10.1175/1520-0493(1995)123<1225:LSCVOT>2.0.CO;2
10. Kuo HL (1965) On the formation and intensification of tropical cyclones through latent heat released by cumulus convection. Am Meteorol Soc 22 1:40-63. https://doi.org/10.1175/1520-0469(1965)022<0040:OFAIOT>2.0.CO;2

11. Lazenby MJ, Todd MC, Wang Y (2016) Climate model simulation of the South Indian Ocean Convergence Zone: mean state and variability. Clim Res 68 1:59–71. https://doi.org/10.3354/cr01382
12. Lemus-Canovas M, Lopez-Bustins J, Trapero L, Martin-Vide J (2019a) Combining circulation weather types and daily precipitation modeling to derive climatic precipitation regions in the Pyrenees. Atmos Res 220:181–193. https://doi.org/10.1016/atmosres.2019.01.018.
13. Loriaux JM, Lenderink G, Siebesma P (2017) Large-scale controls on extreme precipitation. J Clim 30 3:955-968. https//doi.org/10.1175/JCLI-D-16-0381.1
14. Maheras P, Kolyva-Machera F (1990) Temporal and spatial characteristics of annual precipitation over the Balkans in the twentieth century. Int J Climatol 10 5:495-504. https://doi.org/1002/joc.3370100506
15. Maraun D, Widmann M (2018) Statistical Downscaling and Bias Correction for Climate Research. Cambridge: Cambridge University Press 9781107588783. https://doi.org/1017/9781107588783
16. Martin-Vide J, Sanchez-Lorenzo A, Lopez–Bustins J, Cordobilla MJ, A Garcia-Manuel, Raso JM (2008) Torrential rainfall in the northeast of the Iberian Peninsula: synoptic patterns and WeMO influence. Adv Sci Res 2 1:99–105. https://doi.org/10.5194/asr-2-99-2008
17. Moleteni F, Tibaldi S, Palmer TN (1990) Regimes in the wintertime circulation over northern extratropics. I: observational evidence. Q J R Meteorol Soc 116 49:31-67. https://doi.org/10.1002/qj.49711649103
18. Munday C, Washington R (2017) Circulation controls on Southern Africa precipitation in coupled models: The role of the Angola low. J Geophys Res-Atmos 122 2:861-877. https://doi.org/10.1002/2016JD025736
19. Ninomiya K (2008) Similarities and differences among the South Indian Ocean convergence zone, North American convergence zone, and other subtropical convergence zones simulated using an AGCM. J Meteorol Soc Jpn 86 1:141–165. https://doi.org/10.2151/jmsj.86.141
20. North Gerald, Bell T, Cahalan FR, Moeng FJ (1982) Sampling errors in the estimation of empirical orthogonal functions. Monthly Mon Wea Rev 110 7:699-706. https://doi.org/10.1175/1520-0493(1982)110<0699:SEITEO>2.0.CO;2
21. Plavcova E, Kysely J, Stepanek P (2013) Links between circulation types and precipitation in Central Europe in the observed data and regional climate model simulations. Int J Climatol 34 9:2885–2898. https://doi.org/1002/joc.3882
22. Polade SD, Pierce DW, Cayan DR, Gershunov A, Dettinger DM (2014) The key role of dry days in changing regional climate and precipitation regimes. Sci Rep 4 1: 4364. https://doi.org/1038/srep04364
23. Preisendorfer RW, Zwiers FW, Barnett TP (1981) Foundations of principal component selection rules. Scripps Institute of Oceanography, La Jolla, California, SIO Ref. Series 81-4 (NTIS PB); 83–146613
24. Reason CJC, Mulenga H (1999) Relationships between South African rainfall and SST anomalies in the southwest Indian Ocean. Int J Climatol 19 15:1651–1673. https://doi.org/10.1002/(SICI)1097-

0088(199912)19:15<1651::AID-JOC439>3.0.CO;2-U

25. Reason CJC (2001) Evidence of the influence of the Agulhas Current on regional atmospheric circulation patterns. J Clim 14 12:2769-2778. https://doi.org/10.1175/1520-0442(2001)014<2769:EFTIOT>2.0.CO;2
26. Reason CJC, Smart S (2015) Tropical Southeast Atlantic warm events and associated rainfall anomalies over Southern Africa. Front Environ Sci 3:24. https://doi.org/10.3389/fenvs.2015.00024
27. Richman MB (1981) Obliquely rotated Principal Components: an improved meteorological map typing technique? J Appl Meteorol 20 10:1145–1159.https://doi.org/10.1175/1520-0450(1981)020<1145:ORPCAI>2.0.CO;2
28. Richman MB, Lamb PJ (1985) Climatic pattern analysis of three and seven-day summer rainfall in the Central United States: some methodological considerations and regionalization. J Climate Appl Meteor 24 12:1325–1343. https://doi.org/10.1175/1520-0450(1985)024<1325:CPAOTA>2.0.CO;2
29. Richman MB (1986) Rotation of principal components. J Climatol 6 3:293-335. https://doi.org/10.1002/joc.3370060305
30. Richman MB, Gong X (1999) Relationships between the definition of the hyperplane width to the fidelity of principal component loadings patterns. J Clim 12 6:1557–1576. https://doi.org/10.1175/1520-0442(1999)012<1557:RBTDOT>2.0.CO;2
31. Seibert P, Frank A, Formayer H (2007) Synoptic and regional patterns of heavy precipitation in Austria. Theor Appl Climatol 87 1:139-153. https://doi.org/10.1007/s00704-006-0198-8
32. Sylla MB, Giorgi F, Ruti PM, Calmanti S, Dell'Aquila D (2011) The impact of deep convection on west African summer monsoon climate: a regional climate model sensitivity study.Q J R Meteorol Soc 137 659:1417-1430. https://doi.org/10.1002/qj.853
33. Tyson PD (1986) Climatic change and variability in Southern Africa. Oxford University Press, Capetown
34. Vicente-Serrano SM, López-Moreno JI (2006) The influence of atmospheric circulation at different spatial scales on winter drought variability through a semi-arid climatic gradient in Northeast Spain. Int J Climatol 26 11:1427-1453. https://doi.org/10.1002/joc.1387
35. Vigaud N, Richard Y, Rouault M, Fauchereau N (2009) Moisture transport between the South Atlantic Ocean and Southern Africa: relationships with summer rainfall and associated dynamics. Clim Dyn 32 1:113-123. https://doi.org/1007/s00382-008-0377-7
36. Walker ND (1990) Links between South African summer rainfall and temperature variability of the Agulhas and Benguela Current systems. J Geophys Res Oceans 95 C3:3297-3319. https://doi.org/10.1029/JC095iC03p03297
37. Wilks DS (2006) Statistical methods in the atmospheric sciences, second edition. Int Geophys Ser. ISBN 13: 978-0-12-751966-1

Figures

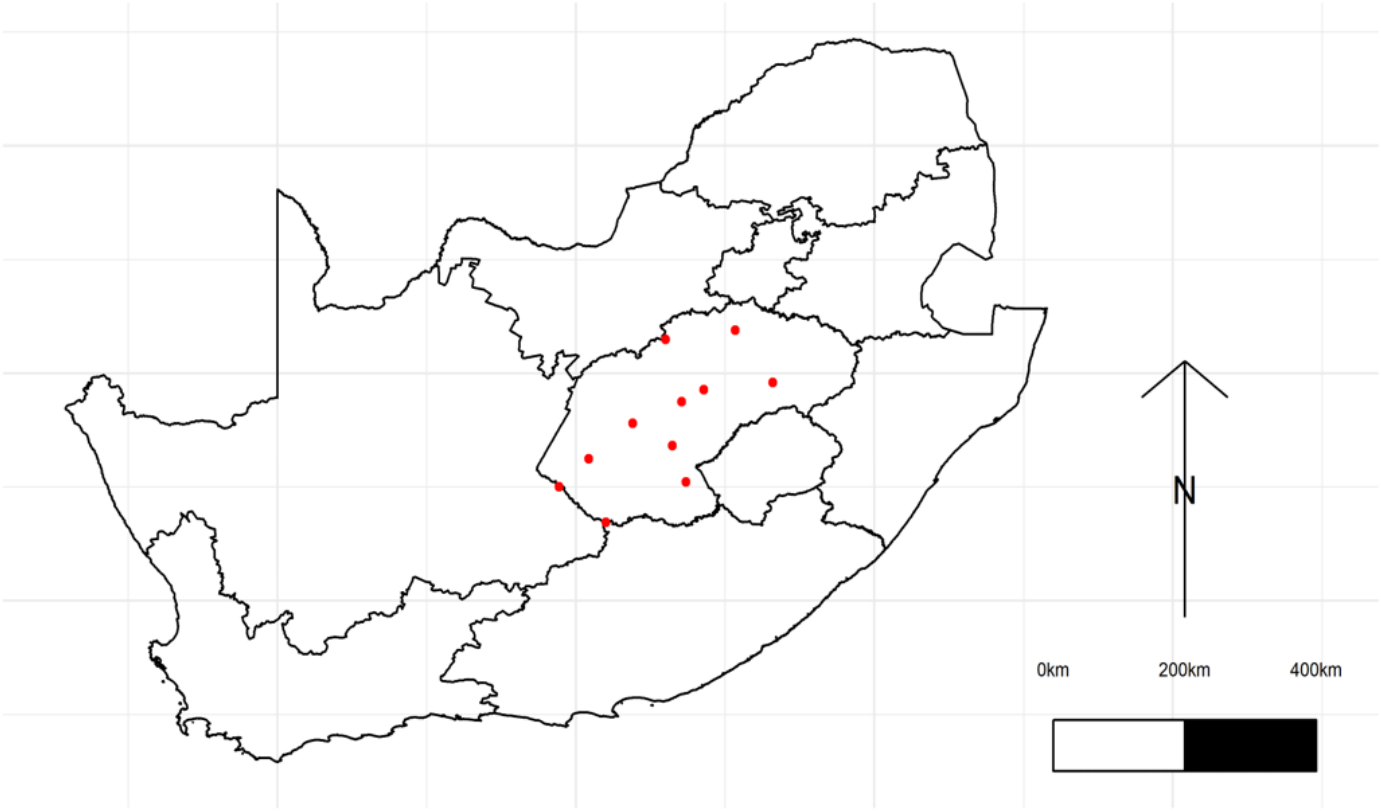

Figure 1

The location of the local study region, Free State, in South Africa. The red dots are the location of the 11 selected rainfall stations in Free State

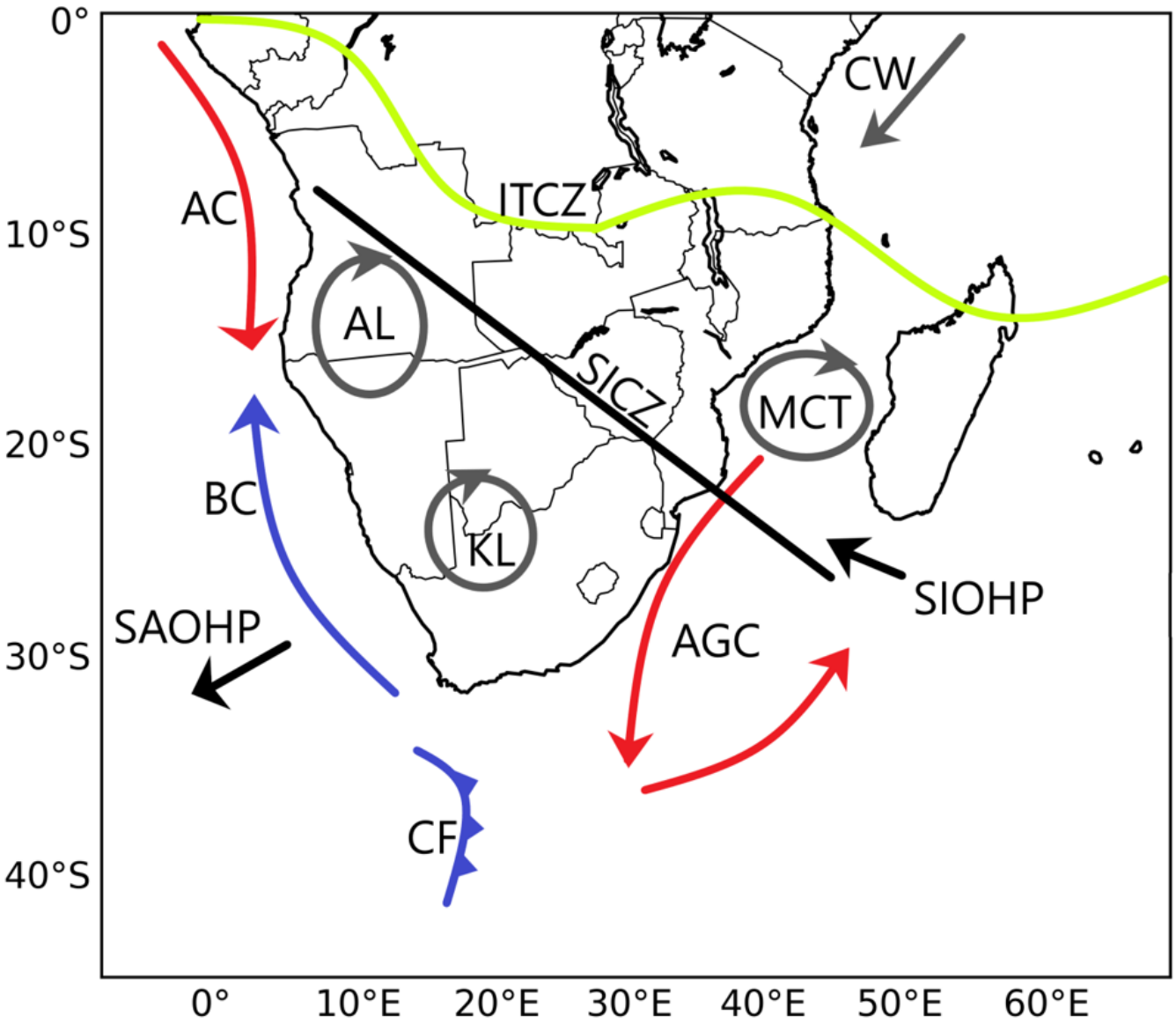

Figure 2

Typical locations of some rainfall producing synoptic systems in Africa, south of the equator. AC: Angola warm current. BC: Benguela cold current. AGC: Agulhas warm current and its retroflection. SIOHP: South Indian Ocean high-pressure. SAOHP: South Atlantic Ocean high-pressure. AL: Angola low. KL: Kalahari low. MCT: Mozambique Channel Trough. CF: cold fronts. ITCZ: Inter-Tropical Convergence Zone. CW: cross-equatorial northeast trade wind. SICZ: South Indian Ocean Convergence Zone. The black arrows at the South Indian Ocean high-pressure and the South Atlantic Ocean high-pressure indicate that the anti-cyclonic circulation at both systems typically drives moisture onshore and offshore southern African landmasses respectively

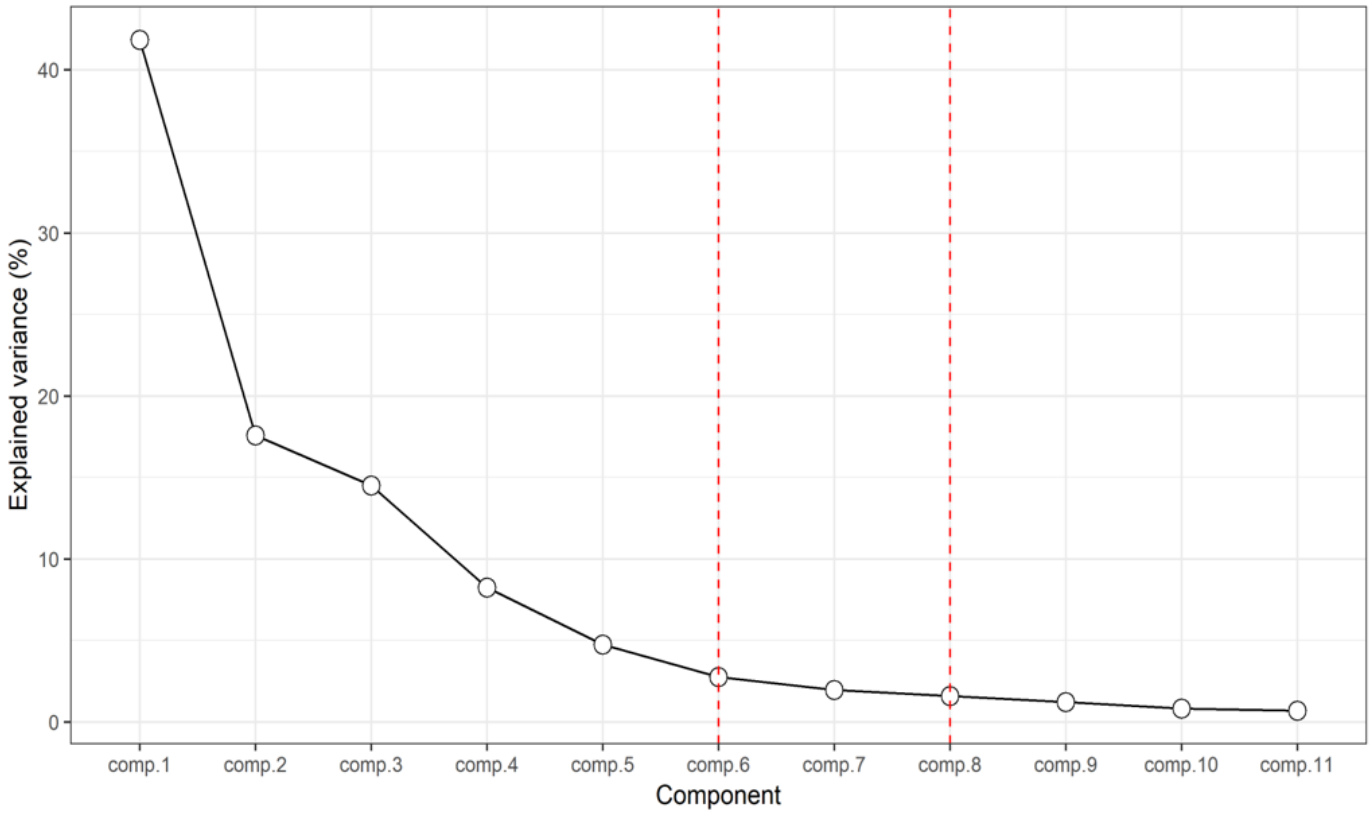

Figure 3

Scree-graph for the PCA analysis. The two red lines demarcate the range of possible component numbers from which truncation can be considered. The x-axis is for the component numbers and the y-axis is the percentage of explained variance by each component

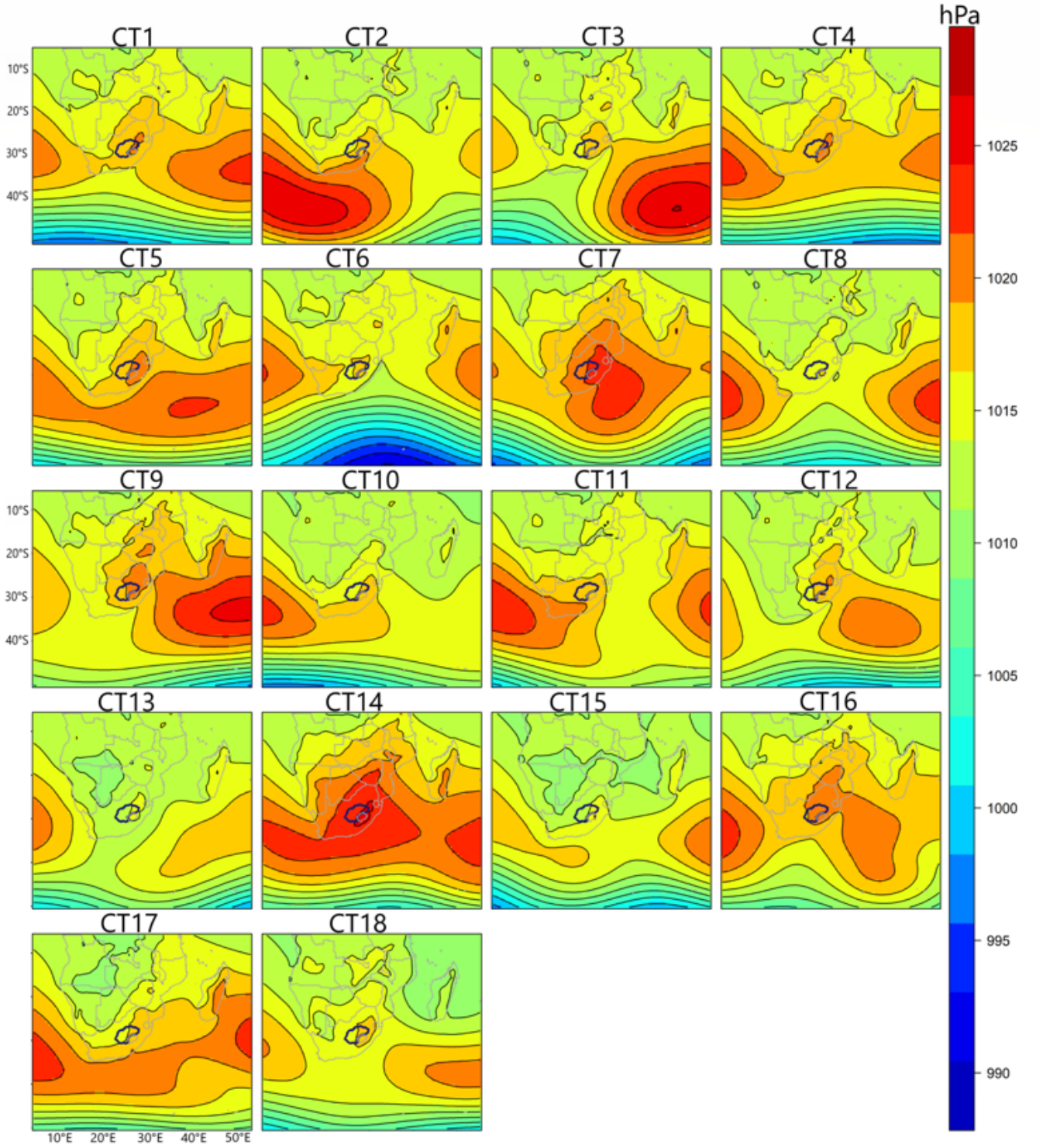

Figure 4

The leading SLP composites (circulation types) in the study region. The blue polygon shows the location of Free State in the maps

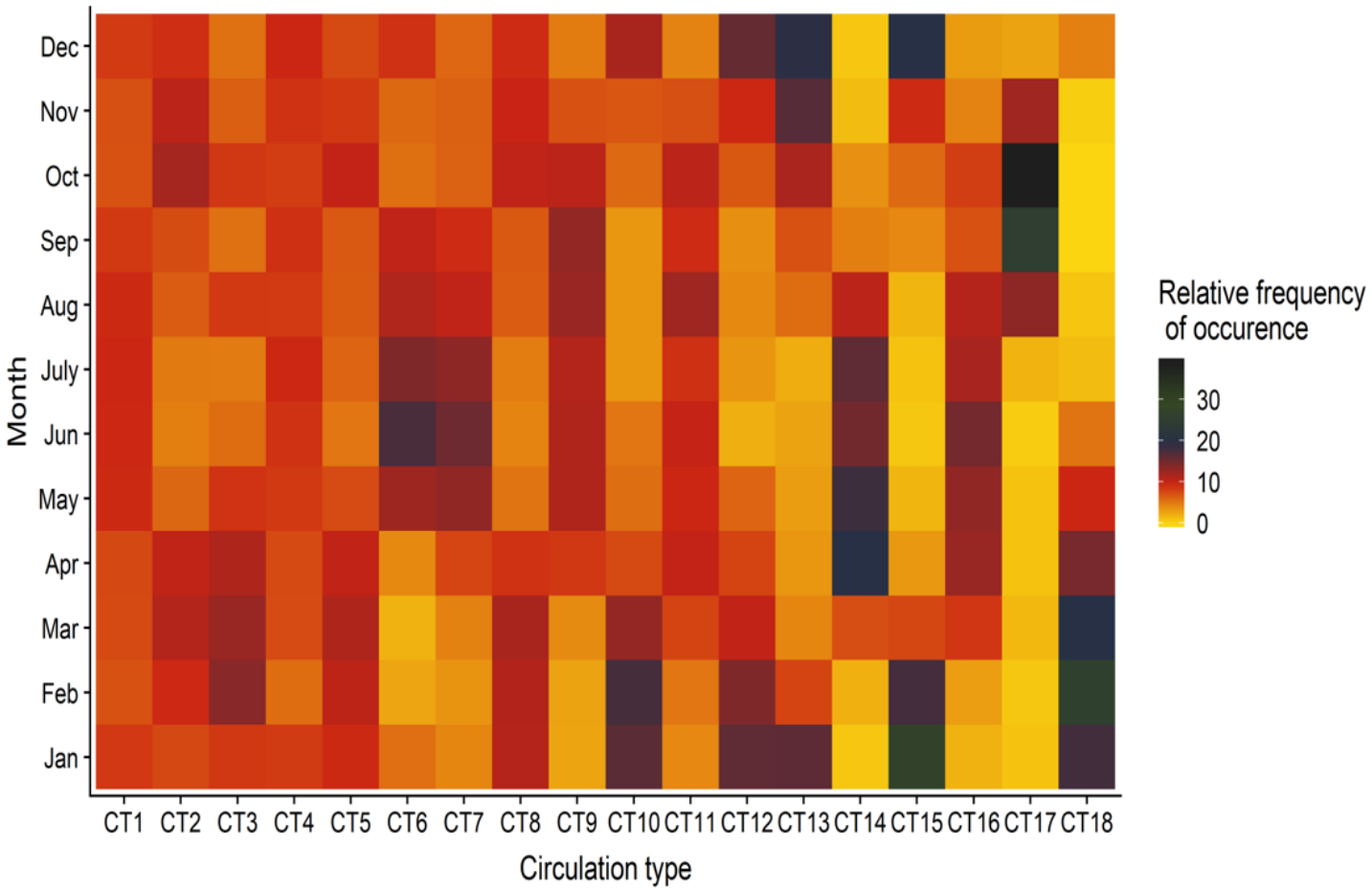

Figure 5

Monthly relative frequency of occurrence (in percentage) for each CT for the 1979-2018 period

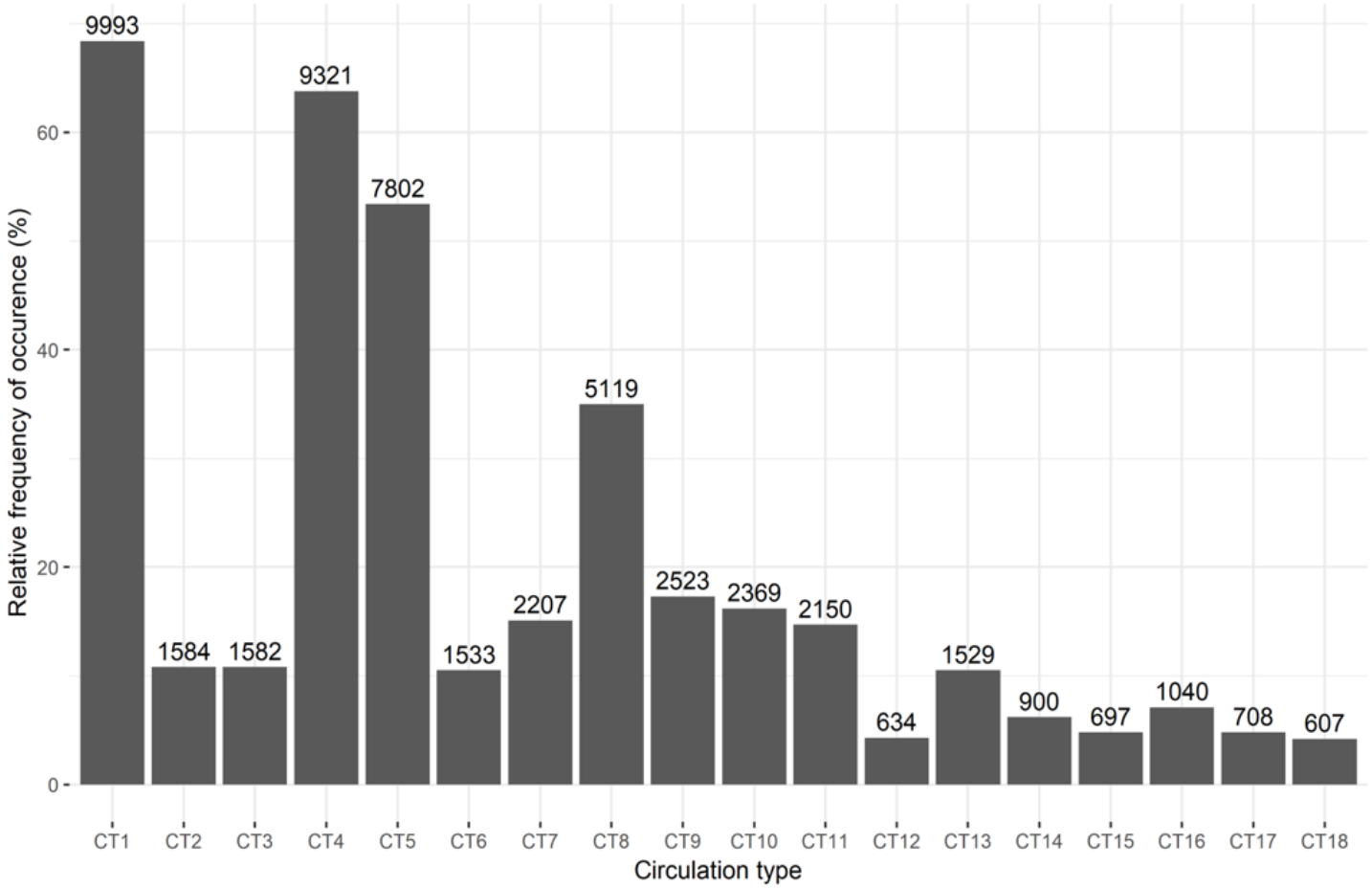

Figure 6

Probability of occurrence of the CTs for the 1979-2018 period. The values on top of the bars are the number of days clustered under each CT

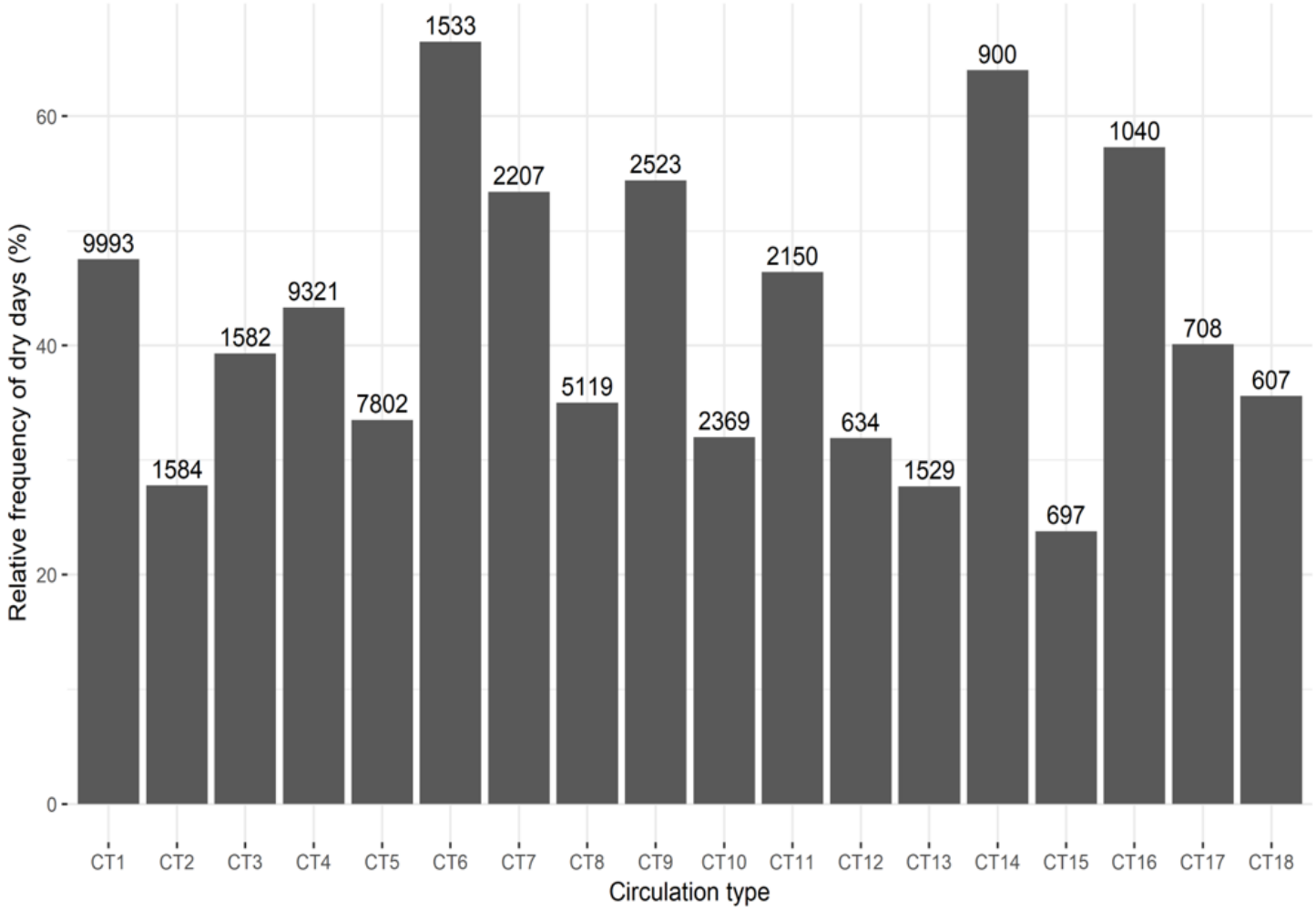

Figure 7

Percentage of dry days in the CTs. The values on top of the bars are the number of days clustered under each CT

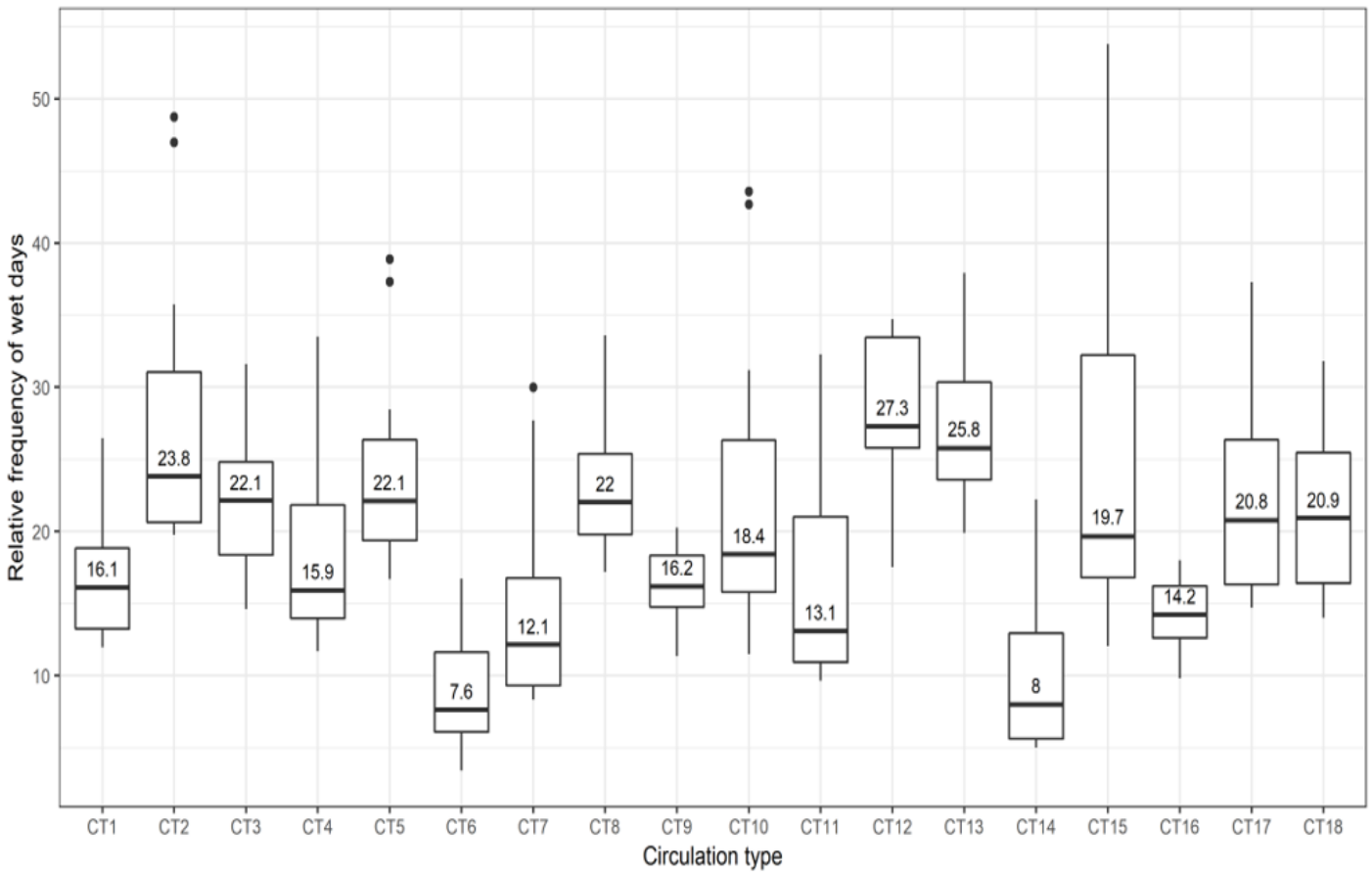

Figure 8

Distribution of the probability of wet days in the eleven stations under each CT. The number in the box-plot is the median of the probability of wet days (in percentage) across the eleven stations. The y-axis is the relative frequency (probability) of wet days for each CT (expressed in percentage)

a)

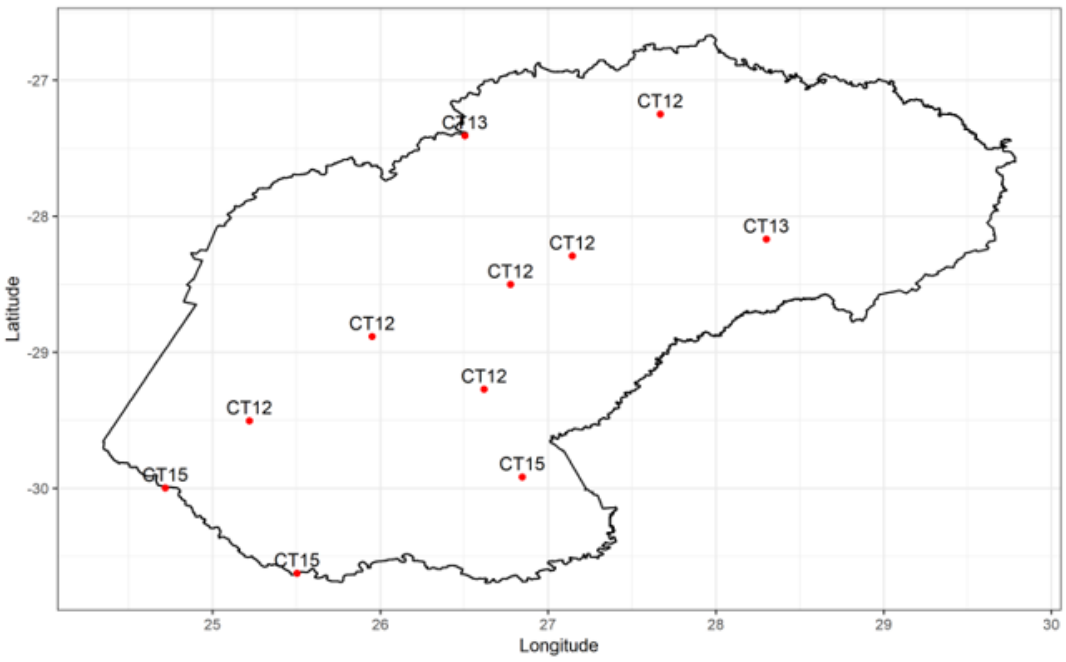

b)

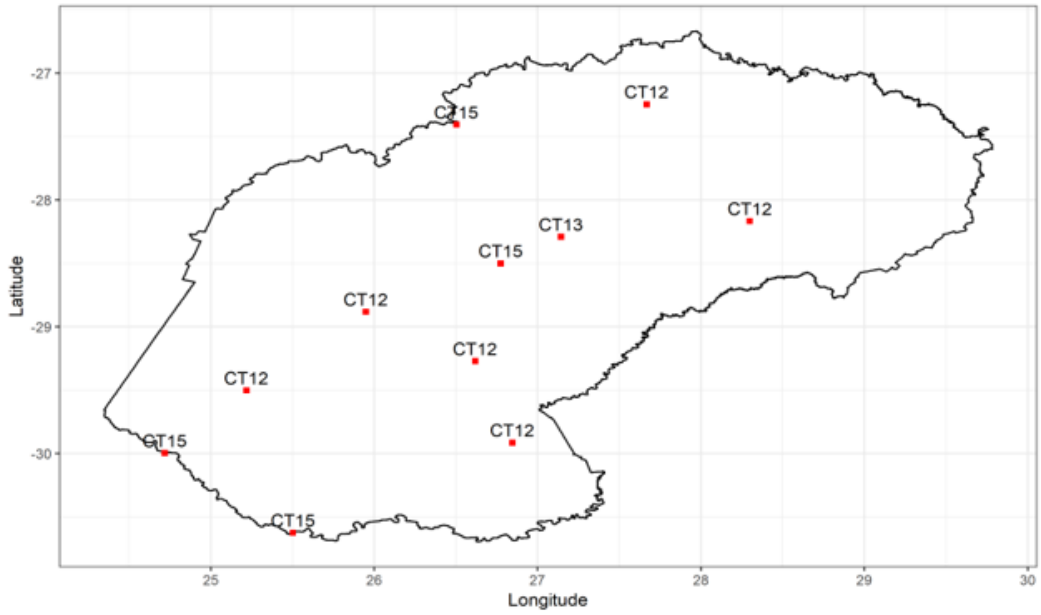

Figure 9

Analysis of the CT with the highest probability of wet days (a) and extreme rainfall days (b) at each of the selected stations

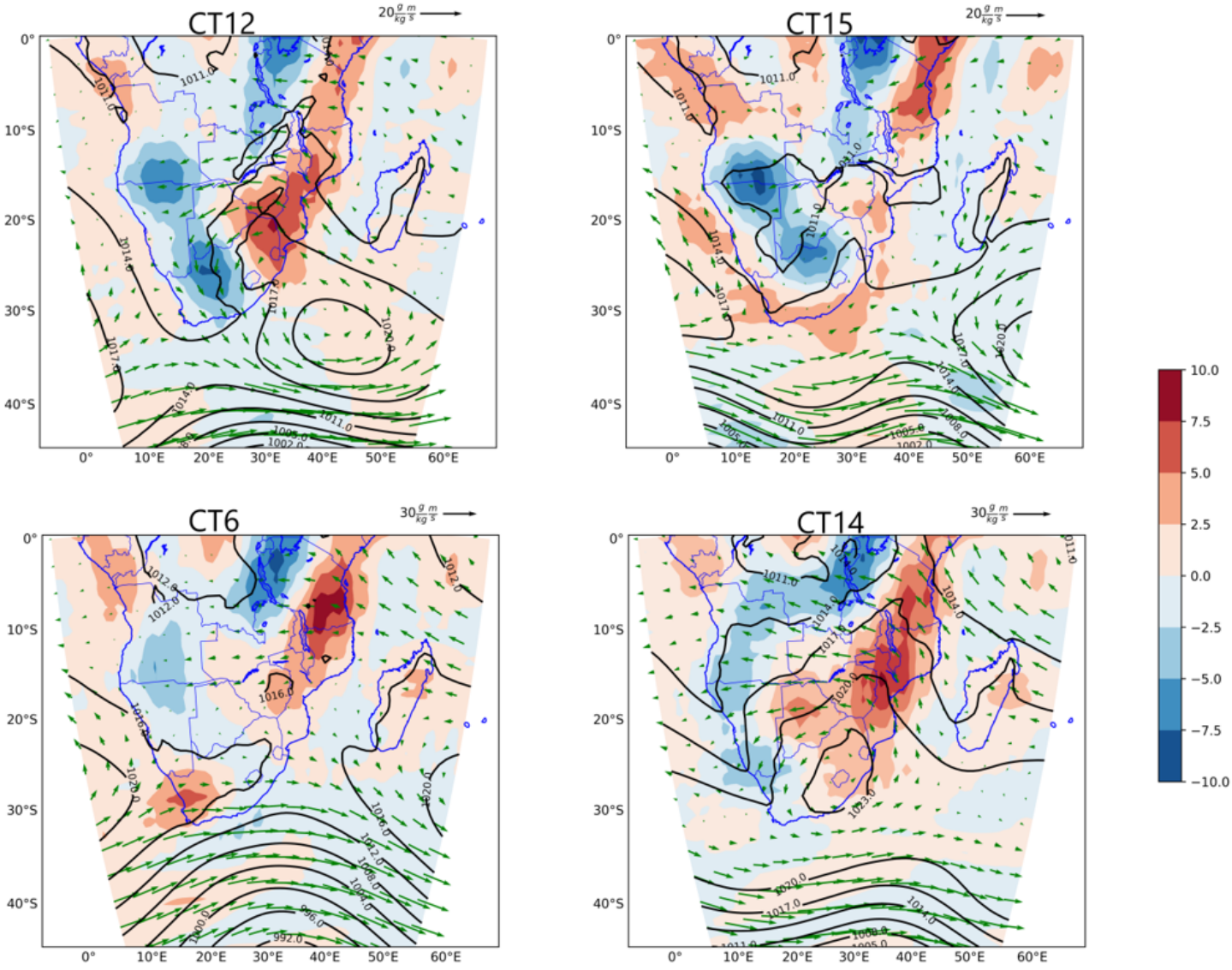

Figure 10

Physical mechanism associated with the CTs with the highest probability of wet days and dry days in Free State. Color bar is the composite of the divergence field for each CT with the unit in 10^6/s ; the green vector is moisture flux in gm/kgs. Vector scale is written on top of the maps